MATHEMATICAL MODELLING OF CHEMICAL REACTION WITH PROPANE

Harijs Kalis[1], Ilmars Kangro[2]
[1]Institute of Mathematics and Computer Science, University of Latvia, Latvia;
[2]Rezekne Academy of Technologies, Latvia
harijs.kalis@lu.lv, ilmars.kangro@rta.lv

Abstract. The main goal of the present study is to promote a more effective use of agricultural residues as an alternative renewable fuel for cleaner energy production with reduced greenhouse gas emissions. The complex experimental study and mathematical modelling of the processes developing during the co-firing of biomass pellets with gaseous fuel were carried out. The experimental study of the effect of co-firing on the main gasification and combustion characteristics was carried out by varying the propane supply and additional heat input into the pilot device with an estimation of the effect of co-firing on the thermal decomposition of pallets. The mathematical model is developed using the environment of MATLAB (2-D modelling) and MATLAB package "pdepe" (1-D modelling) with account variations of supplying the heat energy and combustible volatiles into the bottom of the combustor. The dominant exothermal chemical reactions were used to evaluate the effect of co-firing on the main combustion characteristics and composition of products CO_2 and H_2O. The results prove that the additional heat from the propane flame allows control of the thermal decomposition, the formation of volatiles, and the development of combustion dynamics, thus completing the combustion of biomass and leading to cleaner heat energy production.

Keywords: Arrhenius kinetics, laminar axisymmetric flow, PDEs system, reaction-diffusion equations.

1. Introduction

The EU 20/20/20 targets for cleaner energy production [1] have emphasized the significance of utilizing green energy sources like wood and straw residues [2; 3]. However, using straw for heat production can lead to problems. To tackle this issue, fuel mixture combined combustion processes have been developed that enable the co-combustion of straw with solid [4; 5], or gaseous fuel additives [6].

Varying fuel proportions in multi-fuel gasification/combustion processes can control emission composition, structure, and deposition on heating surfaces [6]. An experimental study was conducted in [2] to analyze the formation of flame composition and temperature profile downstream of swirling flame flows. In references [7] and [8], the Navier-Stokes equations are modified for both viscous, incompressible flows and ideal, compressible flows by incorporating a simple exothermal chemical reaction through the combustion process. This modification eliminates the pressure term in the equations. The experiment involves a cylindrical pipe with swirling flow having axial and azimuthal components of velocity at the inlet. A similar experiment is also described in reference [9].

In reference [10], a study was conducted to model the combustion process with Arrhenius kinetics. The model considers a single-step exothermal chemical reaction between fuel and oxidant in a cylindrical pipe, taking into account the electrodynamical effects due to the Lorentz force action on the combustion process. The study analyzed a non-stationary system of partial differential equations consisting of three components – density, velocity, concentration of fuel, and temperature. It was found that increasing the electrodynamical force leads to an increase in the maximal gas flow velocity and temperature.

In [11], two exothermic reactions for the combustion of H_2 and CO were proceeded for modelling by ANSYS Fluent CFD at the Institute of Physics of the University of Latvia.

The simulations gave an insight into the combustion process in cases when the proportion of the volatiles (H_2, CO) corresponds to that of the biomass consisting of wood or wheat straw, or peat, giving the temperature and velocity distributions in the flame. The maximum flame temperature for the specified ratios 1:1 of the volume fraction of these chemical substances in the fuel mixture was obtained.

The purpose of this paper is to extend the previous research by studying 1-D and 2-D laminar, axially symmetric swirling flow interacting with propane combustion in a chemical reaction process.

2. Materials and methods

The dominant exothermal chemical reaction was used to evaluate the effect of co-firing on the main combustion characteristics and composition of the products CO_2 and H_2O using the propane frame.

For mathematical modelling, the 1-D distribution of an axial component of velocity u_z, density ρ, mass fractions for different species, and temperature T has been calculated with MATLAB solver "pdepe" of the nonlinear parabolic type system of ODEs, depending on the time t and the axial coordinate z for 6-9 unknown functions. For the 2-D model, the approximation is based on the implicit finite-difference and alternating direction method (ADI) of Douglas and Rachford (1956) [12; 13].

2.1. Mathematical modelling of the chemical reactions of propane and oxygen

Based on the experimental measurements, the average concentrations of propane C_3H_8 were used in a mathematical model to determine the concentrations of final products, which include hydrogen H_2, oxygen O_2, and carbon dioxide CO_2. The model considered the exothermic chemical reaction [7]: $C_3H_8 + 5O_2 \rightarrow 3CO_2 + 4H_2O$. This reaction involves two reactants: propane and oxygen, and four species in total.

The 1-D distribution of the combustion mixture includes: a) The axial component of velocity $w = u_z/U_0, (U_0 = 0.1\ \mathrm{m \cdot s^{-1}})$; b) Density $\rho/\rho_0, (\rho_0 = 1\ \mathrm{kg \cdot m^{-3}})$; c) Temperature $T/T_0, (T_0 = 300\ \mathrm{K})$; d) Mass fractions for species $C_k, k = \overline{1,K}$: $K = 4, C_1(C_3H_8), C_2(O_2), C_3(CO_2), C_4(H_2O)$.

The above-mentioned components were computed using a nonlinear parabolic type system of partial differential equations. The calculation was done concerning the time t/t_0, (t_0 = 1 s), and the axial coordinate $x = z/z_0, (z_0 = 0.1\ \mathrm{m})$. This was achieved using the MATLAB routine "pdepe" for K + 3 unknown functions.

At the inlet of the combustor, $x = 0: T = T_0, u_z = U_0, \rho = \rho_0$, the reactants' sum is equal to unity, but the products' sum is zero.

The production rate of the k-th species for a single reaction can be expressed as shown in equation [14]:

$$\Omega_k = \left[(\nu_k'' - \nu_k')R(T)\prod_{n=1}^{K}\left(\frac{\rho C_n}{m_n}\right)^{\nu_n'}\right], k \in [1, K].$$

$R(T)$ is the rate constant for a chemical reaction $R(T) = A'T^{\beta}\exp(E/RT)$ forward path and is modified by Arrhenius temperature dependence.

The other quantities that fall into the expression of the reaction production rate are [13]: A' – the reaction–rate pre–exponential factor; R = 8.314 J·(mol K)$^{-1}$ – the universal gas constant; ν_k'', ν_k' – the corresponding stoichiometric coefficients of the k–th species appearing as a product and reactant in the reaction; β – the order for the temperature; $m_n\ \mathrm{g \cdot m^{-3}}$ – the molecular weigth of the species C_n $(O_2 = 32, CO_2 = 44, H_2O = 18, C_3H_8 = 44)$.

In the equation for mass fractions of the concentrations C_k, the source term is $m_k\Omega_k/\rho\ s^{-1}$. However, in the equation for the temperature, it is correspondingly $\frac{1}{m\rho c_p}\sum_{k=1}^{K} h_k m_k \Omega_k\ \mathrm{K \cdot s^{-1}}$, where $m = \frac{1}{K}\sum_{k=1}^{K} m_k$ is the average molecular weight of the mixture, $c_p = 1000\ \mathrm{J \cdot (kg\ K)^{-1}}$ is the specific heat at constant pressure, $h_k\ \mathrm{KJ \cdot mol^{-1}}$ is the specific enthalpy of the k-th species: $O_2 = 0$, $CO_2 = -394, H_2O = -242, C_3H_8 = -105$.

2.2. 2-D mathematical model

In [13], a model was presented for 2-D axially-symmetric, ideal, laminar compressible swirling flow with propane combustion in a coaxial cylindrical pipe with the following parameters (the cylindrical coordinates (r, z), the time t, $t \in [0, t_f]$, t_f – the end time, the radius $r_0 = 0.05$ m, the length $z_0 = 0.1$ m, the radial component of velocity $u_r\ \mathrm{m \cdot s^{-1}}$). The model is described by four Euler hydrodynamic flow equations and four reaction-diffusion dimensionless equations.

The equations were converted into dimensionless form by scaling all the lengths to a reference length r_0. The other components also were converted into dimensionless form by scaling [13]: a) The meridian velocity to $U_0 = 0.1\ \mathrm{m \cdot s^{-1}}$; b) The azimuthal velocity $v_{\emptyset}$ to $V_0 = 0.3\ \mathrm{m \cdot s^{-1}}$; c) The

temperature to $T_0 = 300\,\mathrm{K}$; d) The density to $\rho_0 = 1\,\mathrm{kg}\cdot\mathrm{m}^{-3}$; e) The pressure to $\rho_0 U_0^2$, $x = z/r_0, w = u_z/U_0, u = u_r/U_0, v = rv_\varphi, p = \rho T$.

The ideal gas equation of state, $p = \rho T$, has been applied, where p is the dimensionless pressure.

We are considering a scenario where a laminar flame with a steady, low speed of ($U_0 = 0.1\,\mathrm{m}\cdot\mathrm{s}^{-1}$) exists in a straight pipe in its base state. The boundary conditions for C_1, C_2 at the inlet ($x = 0$) are as follows: $C_{10} = \overline{0.2,0.6}(C_3H_8), C_{20} = 1 - C_{10}(O_2)$.

Based on the other algorithm [7], we can derive the following results:

$$\frac{C_1}{C_2} = \frac{44}{5\cdot 32} = \frac{11}{40}, C_1 + C_2 = 1, \text{or } C_{10} = 0.22, C_{20} = 0.78.$$

2.3. 1-D mathematical model

Two parabolic-type partial differential equations were considered for 1-D compressible reacting swirling flow and density model in dimensionless form [15], [16].

$$\begin{cases} \frac{\partial \rho}{\partial t} + M(\rho) + \rho\frac{\partial w}{\partial x} = e\frac{\partial^2 \rho}{\partial x^2} \\ \frac{\partial w}{\partial t} + M(w) = -\frac{\partial p}{\rho\,\partial x} + Re^{-1}\frac{\partial^2 w}{\partial x^2}, \end{cases} \tag{1}$$

where $M(s) = w\frac{\partial s}{\partial x}$.

The values $s = \rho, w$, $e = 1\cdot 10^{-5}$, $Re = 10000$ are the factors of the artificial viscosity for approximate density and velocity equations.

The boundary conditions for the inlet ($x = 0$) are in the form $\rho = w = 1$. These values are used as initial conditions at $t = 0$. Zero derivative conditions for functions w and ρ have been applied at the outlet.

For mathematical modelling of one reaction for four chemical species and the temperature, we have the following nonlinear PDEs:

$$\begin{cases} \frac{\partial T}{\partial t} + M(T) = \frac{P_0}{\rho}\frac{\partial^2 T}{\partial x^2} + q_1\rho^5 A_1 T^{\beta_1} C_1 C_2^5 \exp\left(-\frac{\delta_1}{T}\right), \\ \frac{\partial C_1}{\partial t} + M(C_1) = P_1\frac{\partial^2 C_1}{\partial x^2} - \rho^5 A_1 T^{\beta_1} C_1 C_2^5 \exp\left(-\frac{\delta_1}{T}\right), \\ \frac{\partial C_2}{\partial t} + M(C_2) = P_2\frac{\partial^2 C_2}{\partial x^2} - 5\rho^5 A_1 T^{\beta_1} m_2/m_1 C_1 C_2^5 \exp\left(-\frac{\delta_1}{T}\right), \\ \frac{\partial C_3}{\partial t} + M(C_3) = P_3\frac{\partial^2 C_3}{\partial x^2} + 3\rho^5 A_1 T^{\beta_1} m_3/m_1 C_1 C_2^5 \exp\left(-\frac{\delta_1}{T}\right), \\ \frac{\partial C_4}{\partial t} + M(C_4) = P_4\frac{\partial^2 C_4}{\partial x^2} + 4\rho^5 A_1 T^{\beta_1} m_4/m_1 C_1 C_2^5 \exp\left(-\frac{\delta_1}{T}\right), \end{cases} \tag{2}$$

where $\beta_1 = 0, Q_1 = (m_1 h_1 + 5m_2 h_2 - 3m_3 h_3 - 4m_4 h_4)/(m_1 m)$.

The following symbols and constants are used in the partial differential equations, the explanation of which is provided in the literature sources [17]:

$A_1 = A_1'\rho_0^5 z_0/(U_0 m_2^5)$ - the scaled reaction-rate pre-exponential factor, $A_1' = 14\,\mathrm{m}^{15}\cdot(\mathrm{mol}^5\mathrm{s})^{-1}$; $P_k = D/(U_0 r_0) = 0.01, k = 1(1)4, P_0 = \lambda/(c_p\rho_0 U_0) = 0.05, q_1 = Q_1/(c_p T_0) = 5\,J\cdot kg^{-1}$ - the reactions' heat loss; $\delta_1 = E_1/(RT_0) = 18.75$ - the scaled activation energy; $R = 8.314\,\mathrm{J}\cdot(\mathrm{mol\ K})^{-1}$ - the universal gas constant; $E_1 = 1.2\cdot 10^5\,\mathrm{J}\cdot\mathrm{mol}^{-1}$ [17] - the activation energy; $\lambda = 0.25\,\mathrm{J}\cdot(\mathrm{s\ m\ K})^{-1}$ - the thermal conductivity; $D = 2.5\cdot 10^{-4}\,\mathrm{m}^2\cdot\mathrm{s}^{-1}$ – the species' molecular diffusivity.

The following components of equations were converted into dimensionless form by scaling:

a) all lengths to $r_0 = 0.05\,m$; b) the meridian velocity to $U_0 = 0.1\,\mathrm{m}\cdot\mathrm{s}^{-1}$; c) the temperature to $T_0 = 300\,K$; d) the density to $\rho_0 = 1\,\mathrm{kg}\cdot\mathrm{m}^{-3}$; e) the pressure to $\rho_0 U_0^2$. At the inlet ($x = 0$) the boundary conditions for C_1, C_2 are in the following form:

$C_{10} = \overline{0.1,0.4}(C_3H_8)$, $C_{20} = 1 - C_{10}(O_2)$, (see Tab. 2 for $t_f = 10$,).

Using the other algorithm [10], it is possible to calculate the following results:

$$\frac{C_1}{C_2} = \frac{44}{5 \cdot 32} = \frac{11}{40}, C_1 + C_2 = 1, \text{or } C_{10} = 0.22, C_{20} = 0.78.$$

3. Results and discussion

In this chapter, we will study how the combustion mixture temperature, velocity, and concentration change over time and space using 2-D and 1-D flow models. Our focus will be on identifying the specific values of these parameters at which the mass fraction of propane at the outlet is the lowest.

3.1. Results for the 2-D model

In Table 1 [15] we can see the results of $t_f = 10$, *Mw* = max(*w*), *MT* = max(*T*), *Mu* = max(*u*), $MC3 = \max(C_3), MC4 = \max(C_4), dp = \max(p) - \min(p), mC2 = \min(C_2), Mro = \max(\rho)$. The maximum values of temperature *MT*, velocity *Mw*, pressure *dp*, *MC4*, *MC3* (CO_2, H_2O) are obtained for $C_{10} = 0.20; 0.22$, when the outlet's ($x = 2$) propane mass fraction is minimal.

Table 1

Values of *Mw, Mu, MT, MC3*(H_2O), *MC4*(CO_2), *mC2*(O_2), *dp, Mro* depending on C_{10}

C_{10}	MT	Mu	Mw	$MC2$	$MC3$	$MC4$	dp	Mro
0.20	1.87	2.48	3.26	0.20	0.49	0.27	1.67	1.08
0.22	1.87	2.48	3.26	0.19	0.49	0,27	1.67	1.08
0.30	1.81	2.48	3.21	0.16	0.45	0.24	1.65	1.10
0.40	1.69	2.49	3.10	0.16	0.37	0.20	1.59	1.15
0.50	1.55	2.53	2.94	0.18	0.27	0.15	1.50	1.20
0.60	1.06	2.59	2.42	0.35	0.03	0.01	0.90	1.00

3.2. Results for the 1-D model

The numerical results in the domain (x, t) for $x \in [0,2], t \in [0, t_f], t_f = 1; 10$ have been obtained characterizing the result dependence on x, t. During the thermochemical conversion of biomass pellets and their mixtures, the maximum values of temperature, axial flow velocity, and species mass fractions are achieved:

$Mw = \max(w), Tend = T(2, t_f), wend = w(2, t_f)$,

$C1end = C_1(2, t_f), C2end = C_2(2, t_f), C3end = C_3(2, t_f), C4end = C_4(2, t_f)$.

The reactant O_2 mass fraction decreases to zero by $t = t_f$. The maximal values of *MT*, *Mw*, *wend*, *Tend*, *MC4*(CO_2) and *MC3*(H_2O) are obtained at $C_{10} \leq 0.4$ when the mass fraction of propane at the outlet $x = 2$ ($C1end$) is minimal (see Tab. 2).

Table 2

Values of *Mw, wend, MT, Tend, C1end* (C_3H_8), *C2end* (O_2), *C3end* (CO_2), *C4end* (H_2O) depending on C_{10}

C_{10}	Mw	*wend*	MT	$Tend$	$C1end$	$C2end$	$C3end$	$C4end$
0.1	4.48	1.61	4.78	2.11	0.00	0.54	0.30	0.16
0.2	6.64	1.97	8.48	3.67	0.01	0.09	0.59	0.32
0.3	6.41	1.93	7.91	3.52	0.12	0.04	0.54	0.30
0.4	4.10	1.88	7.40	3.61	0.25	0.06	0.45	0.24

At the initial condition value $C_{10} = 0.2$ (the propane mass fraction at the outlet $x = 2, C1end = 0.01$, $\rho(2, t_f) = 0.492$) there were obtained the maximum values of *MT*, *Mw*, *wend*, *Tend*, CO_2, H_2O.

Moreover, at $C_{10} = 0.1$ the mass fraction $C1end = 0$ was obtained, and the mass fraction for oxygen (O_2) was $C2end = 0.54$ (in this case the mass fraction of propane at the inlet turned out to be too small.)

Figs. 1-12 show the interaction of temperature, axial velocity, and concentrations depending on $(x,t)(x \in [0,2], t \in [0,t_f], t_f = 10), C_{10} = 0.4, C_{20} = 0.6$.

In Figures 1 and 2 we can see the distribution of the temperature $T(x,t)$ in the combustion chamber ($x \in [0,2]$, $t \in [0,t_f]$, $t_f = 10$), the temperature increases monotonically with time from the value $1T(x,0) = 1$ to its maximum value $MT \approx 7.40$ at the time $t \approx 1$ on the left side of the combustion chamber, then the temperature decreases to the value $Tend = 3$ at the time value $t = 10$.

The dimensional temperature value in Kelvin degrees is calculated by multiplying the dimensionless temperature value by 300 K.

In Figures 3 and 9 we can see the distribution of propane C_3H_8 mass fraction $C_1(x,t)$ in the combustion chamber ($x \in [0,2]$, $t \in [0,t_f]$, $t_f = 10$). Here, the mass fraction of propane decreases monotonically in a very short time interval – from the value $C_{10} = 0.4$ at the time value $t = 0$ to $C1end \approx 0.25$, and it remains so throughout the subsequent time $t \geq 1$ in the combustion chamber section starting from x ≥ 0.1 to $x = 2$.

In Figures 4 and 10 the distribution of oxygen O_2 mass fraction $C_2(x,t)$ is described. The mass fraction $C_2(x,t)$ decreases from the value $C_{20} = 0.6$ at the time value $t = 0$ to the value $C2end = C_2(0.1,t) \approx 0.06$, and it remains so for the entire subsequent time $t \geq 1$ (Fig. 4).

On the other hand, Figure 10 shows the decrease of $C_2(x,t)$ to the value $C2end = C_2(x,10) \approx 0.06$ in the entire further part of the combustion chamber $x \geq 1$.

In Figures 5 and 7 the distribution of product CO_2 mass fraction $C_3(x,t)$ is described. The mass fraction $C_3(x,t)$ is increasing from zero to $C3end = C_3(0.1,t) \approx 0.45$ and maintains this value throughout the following time $t \geq 1$ (Fig. 5), while Figure 7 shows reaching and maintaining this value $C3end = C_3(x,10) \approx 0.45$ in the combustion chamber part $x \geq 1$.

In Figures 6 and 8 the distribution of product H_2O mass fraction $C_4(x,t)$ is described. The mass fraction $C_4(x,t)$ is increasing from zero to $C4end = C_4(0.1,t) \approx 0.24$ and maintains this value throughout the following time $t \geq 1$ (Fig. 6), while Figure 8 shows reaching and maintaining this value $C4end = C_4(x,10) \approx 0.24$ in the combustion chamber part $x \geq 1$.

In Figure 11 the distribution of the axial velocity $w(x,t)$ is described. It shows that the distribution of the axial velocity $w(x,t)$increases over time from the value $w(0,t) = 1$ to $wend = 1.88$ at the time value $t = 10$. The maximum value $Mw \approx 3.90$ is reached at $t = 1, x = 2$.

Figure 12 describes the distribution of density $\rho(x,t)$. It shows that the density $\rho(x,t)$ increases from the value $\rho(0,t) = 1$ to $\rho(x,1) \approx 2$, then at $t > 1$ the density decreases to the value $\rho(2,10) \approx 0.53$.

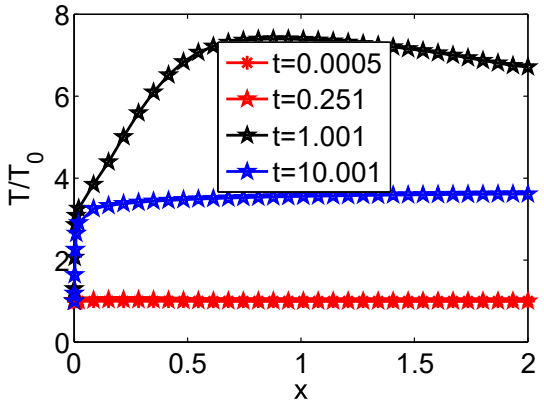

Fig. 1. **Temperature of the combustion mixture depending on x for fixed t, $Tend = 3.6142$**

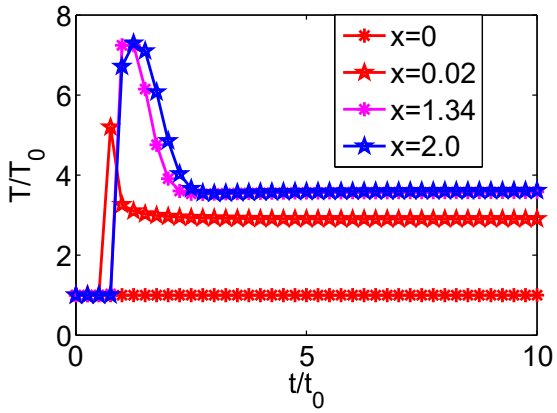

Fig. 2. **Temperature of the combustion mixture depending on t for fixed x, $Tmax = 7.3974$**

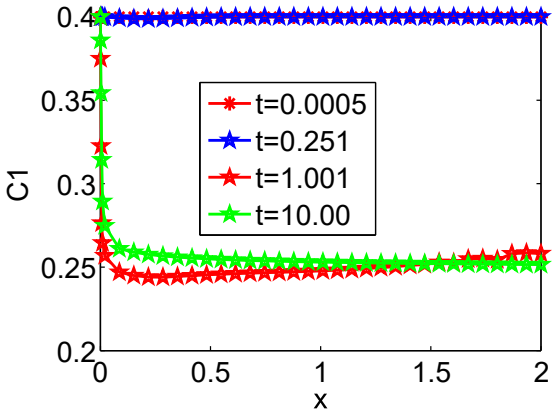

Fig. 3. **Propane C_3H_8 mass fraction vs.x for fixed t, $C1end = 0.2515$**

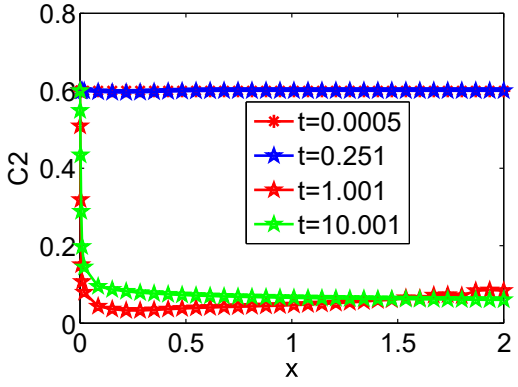

Fig. 4. **O_2 mass fraction vs.x for fixed t, $C2end = 0.0601$**

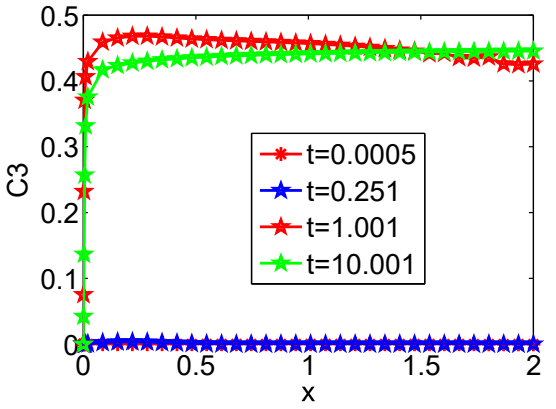

Fig. 5. **CO_2 mass fraction vs.x for fixed t, $C3end = 0.4454$**

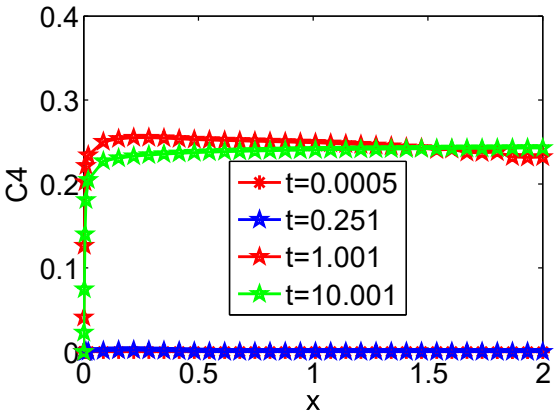

Fig. 6. **H_2O mass fraction vs.x for fixed t, $C4end = 0.2429$**

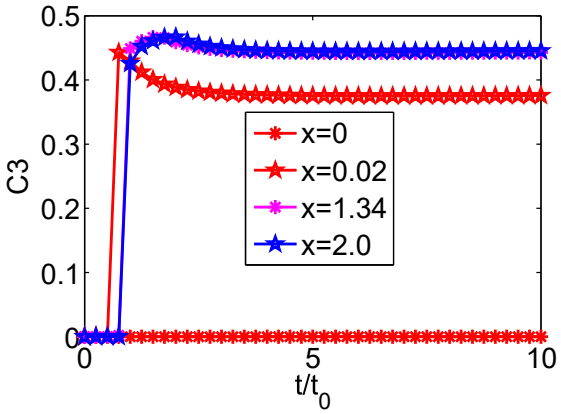

Fig. 7. **CO_2 mass fraction vs.t for fixed x, $C3end = 0.4454$**

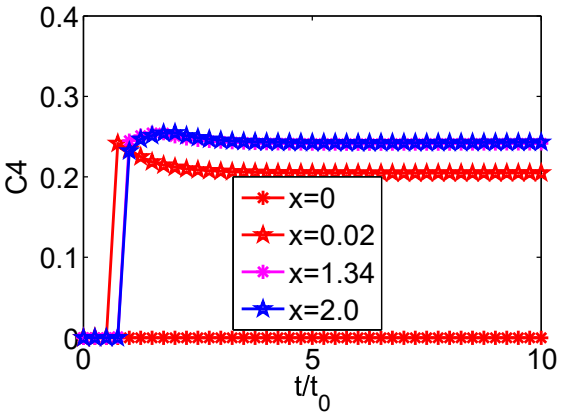

Fig. 8. **H_2O mass fraction vs.t for fixed x, $C4end = 0.2429$**

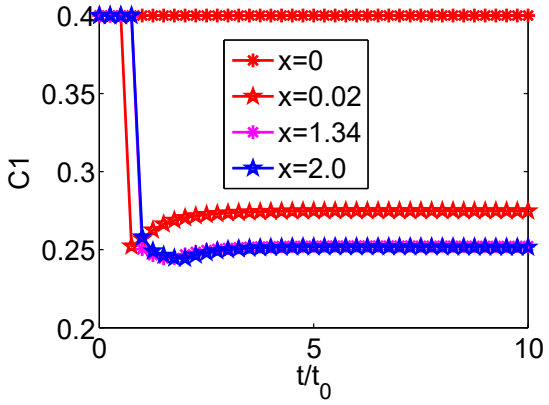

Fig. 9. **Propane C_3H_8 mass fraction vs.t for fixed x, $C1end = 0.2515$**

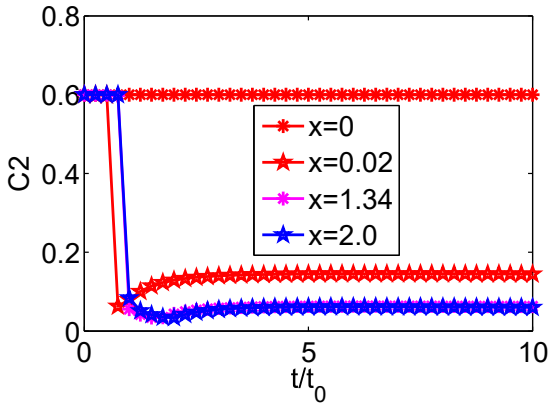

Fig. 10. **O_2 mass fraction vs.t for fixed x, $C2end = 0.0601$**

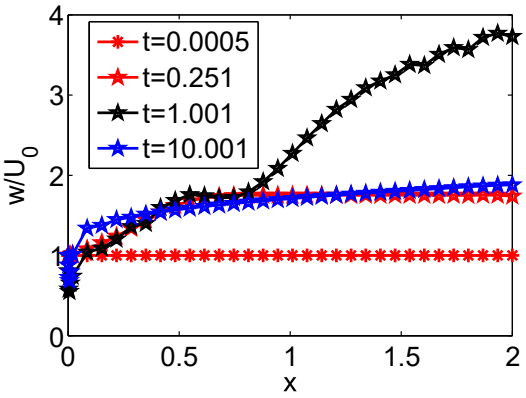

Fig. 11. **Velocity w vs.x for fixed t, $wend = 1.8802$**

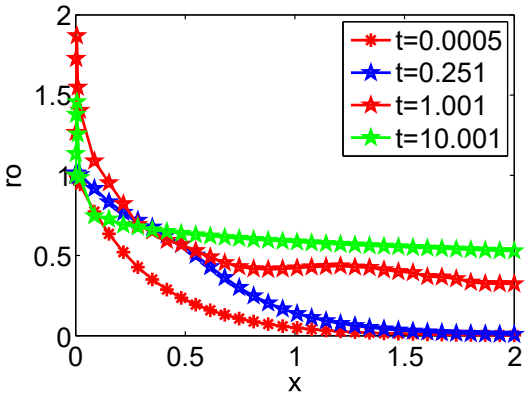

Fig. 12. **Density *ro* vs.x for fixed t, $\rho(2, 10)$ = 0.5286**

Conclusions

1. The chemical reaction has been calculated using Arrhenius kinetics with the help of five partial differential equations (PDEs). Two partial differential equations are used for the 1-D mathematical model of compressible reacting swirling flow and density. For the 2-D mathematical model of axially-symmetric, ideal, laminar compressible swirling flow, 4 Euler hydrodynamic flow equations, and 4 reaction-diffusion equations are used.
2. The maximum values for temperature, velocity, and mass fractions of CO_2 and H_2O are achieved with a propane mass fraction of 0.2 at the inlet. The maximal temperature, velocity, and mass fraction values of products in the combustion mixture are achieved when the propane mass fraction at the outlet is minimized.
3. In the present article it was obtained that for propane injections, maximum values of the temperature, axial velocity and mass fractions of the products CO_2, H_2O are obtained when the mass fraction of O_2 is maximum at the inlet. The concentration of the products increases over time. The mass fraction of the reactants in the reactions at the small-time moment ($t \approx 0.3$ s) decreases, and O_2 decreases to zero for all propane injections. It should also be noted that during the reaction the mass fraction of reactants increases, while the mass fraction of products decreases, at the same time the total sum of the mass fractions of reactants and products remains the same and is equal to 1(with an accuracy of 1 %).
4. At the Institute of Physics of the University of Latvia, research was conducted on the processes that develop in co-combustion of straw with propane. The results of mathematical modeling and experiments showed that the maximum values of the flame temperature, axial flow rate and mass fractions of the main products at the thermochemical reaction, the composition and temperature of

the products at co-firing straw with propane are strongly influenced by the propane supply into the device. Studies have shown that the maximum value of the molar fraction of the products and flame temperature for the stoichiometric combustion conditions can be achieved during the relatively small period ($t < 10\ s$) and refer to the mass fraction of propane $0.2 - 0.4$ at the inlet of the combustor.

5. Comparing the research carried out at the Institute of Physics of the University of Latvia with the results of mathematical modeling obtained in the given publication, it should be concluded that there is a close qualitative correspondence about the proportion of reactants and products of chemical reactions, to the main characteristics of the chemical reaction - the amount of propane in the combustion mixture, the maximum combustion temperature, the reaction time. Therefore, the results obtained in the publication, considering the above-mentioned study, allow optimize the residues of the products of the considered chemical reaction - CO_2 and H_2O, which undoubtedly gives an impetus to new experimental activity.
6. Nonlinear PDEs with chemical reaction are calculated using MATLAB solver “pdepe”. The numerical simulation can provide main combustion parameters for comparison with experimental data, although the mathematical model requires further development.

Author contributions

The contribution of all authors (H.K. and I.K.) to the development of a given publication is equivalent. All authors have read and agreed to the published version of the manuscript.

References

[1] Eu, 2020 Climate and energy package. Climate strategies and targets. http://ec.europa.eu/clima/policies/strategies/2020/index en.htm, 2012.
[2] Barmina I., Lickrastina A., Zake M., Arshanitsa A., Solodovnik A. Telysheva G. Experimental study of thermal decomposition and combustion of lignocellulosic biomass pellets. Latvian Journal of Physics and Technical Sciences, vol. 50, Nr.3, 2013, pp. 35-48.
[3] Vassilev S.V., Baxter D., Andersen L.K., Vassileva Ch.G. An overview of the chemical composition of biomass. Journal Fuel, vol. 89, 2010, pp. 913-933.
[4] U. S. Department of Energy, National Energy Technology Laboratory (NETL). Biomass Cofiring Program. Program Facts, 2000. http://www.netl.doe.gov.
[5] Veijonen, K., Vainikka P., Järvinen T., E., Alakangas E. Biomass co-firing an efficient way to reduce greenhouse gas emissions. European Bioenergy Networks, 2003, pp. 26. http://eubionet,vtt.fi.
[6] Brown M., Judd R.W. Emission reduction through biomass and gas co-firing – the Bagit project. Proceedings of International Conference “23rd World Gas Conference Amsterdam”, Amsterdam, 2006, pp.13.
[7] Kalis H., Marinaki M., Strautins U., Lietuvietis O. On the numerical simulation of the combustion process with simple chemical reaction. Proceedings of International Conference “Baltic Heat Transfer Conference BHTC”, Aug. 24-26, 2015, Tallinn, Estonia, pp. 175-180.
[8] Kalis H., Marinaki M., Strautins U., Lietuvietis O. On the numerical simulation of the vortex breakdown in the combustion process with simple reaction and axial magnetic field. Int. Jour. of Differential Equations and Applications, vol. 14, Nr. 3, 2015, pp. 235-250.
[9] Barmina I., Kolmickovs A., Valdmanis R., Zake M., Kalis H. Experimental and numerical studies of electric field effects on biomass thermo-chemical conversion. Chemical Engineering Transaction, vol. 50, 2016, 121-126.
[10] Kalis H., Marinaki M., Strautins U., Zake M. On numerical simulation of electromagnetic field effects in the combustion process. MMA, vol. 23, Nr. 2, 2018, pp. 324-343.
[11] Barmina I., Valdmanis R., Zake M., Ozola L., Strautins U. Development of gasification/combustion characteristics at thermochemical conversion of biomass mixtures. Proceedings of International Conference “16th Int. Conf. on Engineering for Rural Development”, May 24-26, 2017, Jelgava, Latvia, pp. 54-59.
[12] Douglas J., Rachford R. On the numerical solution of heat conduction problems in two and three space variables. Trans. Amer. Math. Soc., vol. 82, Nr .2,1956, pp. 421-439.

[13] Barmina I., Kalis H., Kolmikovs A., Marinaki M., Ozola L., Strautins U., Valdmanis R., Zake M. Mathematical and experimental study of straw co-firing with gas. MMA, vol. 24, Nr. 4, 2019, pp. 507-519.
[14] Smooke M.D., Turnbull A.A., Mitchella R.E., Keyes D.E. Solution of two-dimensional axisymmetric laminar diffusion flames by adaptive boundary value methods. Journal NATO ASI Series E: Applied Sciences, vol. 140, 1987, pp. 261-300.
[15] Kalis H., Kangro I. Effective finite difference and Conservative Averaging methods for solving problems of mathematical physics. Monography. Rezekne Academy of Technologies, 2021. 423 p. [online] http:\\books.rta.lv/index.php/ RTA/catalog/ book 24.
[16] Kalis H., Kangro I., Gedroics A. Numerical methods of solving some nonlinear heat transfer problems. Int. Journ. of Pure and Applied Mathematics, vol. 57, Nr. 4, 2009, pp. 467-484.
[17] Martinez I. Combustion kinetics. Set of lectures, 2014, pp. 47. [online][11.02.2024] Available at: http://webserver.dmt.upm.es/~isidoro/bk3/c15/Combustion.pdf.